Fermion-Pomeron interactions in a Reggeon field theory

Robert Savit* and Jochen Bartels†
Fermi National Accelerator Laboratory, Batavia, Illinois 60510 ‡
(Received 12 September 1974)

A Reggeon field theory which describes the interaction of a Pomeron with a pair of fermions of opposite parity is studied using the renormalization group and the ϵ expansion. In the infrared limit a solution is found with a number of physically attractive features. The renormalized fermion trajectories are nearly proportional to u for small u even though the bare trajectories were proportional (for small u) to $\sqrt{u}$. Furthermore, both renormalized parity poles are on the physical j-plane sheet for $u < 0$, but one of them moves under a cut for $u > 0$ and does not appear as a physical particle—all this despite the fact that the bare theory has physical fermions of both parities. Phenomenological implications for backward π-N scattering, and implications for the general structure of Reggeon field theories are also discussed.

I. INTRODUCTION

It is now generally known that for a Regge description of high-energy processes, the exchange of a simple pole must *a priori* be corrected by additional Pomeron exchange. If the Pomeron has intercept 1, this leads to branch cuts in the angular momentum plane, which at $t=0$ accumulate at the intercept of the pole. When summing up all these corrections, the resulting j-plane singularity may be very different from the simple pole. A technique for the examination of such Reggeon-Pomeron interaction is Gribov's Reggeon calculus.[1] In this scheme one constructs a field theory in two space dimensions (transverse momentum) and one time dimension (angular momentum). The solution of this field theory should describe the j-plane structure of the complete Reggeon-Pomeron interaction. Such field theories were studied several years ago by Gribov and others.[2] Their approach was primarily perturbative, although they did deduce some properties of the exact solution.

Recently, substantial progress has been made in applying renormalization-group techniques to these theories. A number of models for the interaction of the Pomeron with itself[3] have been studied in this way, as well as a theory in which a boson trajectory interacts with a Pomeron.[4] The results of these studies strongly indicate that the renormalized Pomeron or boson singularity which contains the complete interaction with the Pomeron is considerably different from what it was without the interaction.

In the present paper we shall use the renormalization group to examine a Reggeon field theory with a fermion and a Pomeron. A theory similar to ours was studied some time ago by Gribov, Levin, and Migdal,[5] but the recent results on the Pomeron renormalization indicate a necessity to reconsider the fermion problem. Indeed, our results differ substantially from those of Ref. 5.

A careful study of the fermion trajectory is of particular interest not only because of its role in high-energy physics, but also because the Reggeization of fermions has for many years been plagued with apparent inconsistencies. In backward π-N scattering, the assumption of Mandelstam analyticity for the A and B amplitudes implies a symmetry, the MacDowell symmetry, between the u-channel partial-wave amplitudes.[6] If backward π-N scattering is dominated by the exchange of fermion Regge poles, this symmetry requires the existence of two poles of opposite parity whose trajectories are related by

$$\alpha_+(\sqrt{u}) = \alpha_-(-\sqrt{u}). \tag{1.1}$$

This suggests that the natural variable for the trajectories to depend on is $\sqrt{u}$ rather than u. Experimentally, however, it seems that the nucleon trajectory is almost linear in u, and thus it is rather puzzling that the negative-parity nucleons, which should be almost degenerate with the well-known ones of positive parity, have not been seen. To date, no satisfactory dynamical mechanism has been proposed to explain the absence of these parity doublets.

In comparison with boson Reggeization, the problem of fermion Reggeization seems to be in a state of rather deep confusion. It would certainly be desirable to construct a theory which would help us see the order underlying this chaos, and it is to the description of such a theory that we now turn.

The concept of a Reggeon field theory that we use in this paper will be the same as in the earlier studies of the pure Pomeron and the boson-Pomeron interactions. In defining our theory, we have *a priori*, considerable freedom since we are free to choose the energy-momentum relations of the

field, as well as their interactions. The theory we consider contains a Pomeron and a pair of fermions. Both the Pomeron and the fermion are allowed to emit and absorb Pomerons, so that our chosen Lagrangian contains two kinds of cubic couplings. Consistent with the usual ideas about absorption and Gribov's analysis of signature, the coupling constants are taken to be purely imaginary.

Because it is in some sense (not, as it turns out calculationally) the simplest choice, we assume for the bare Pomeron a linear pole,

$$\alpha_0(u) = 1 + \alpha_0' u\,, \tag{1.2}$$

and for the bare positive- and negative-parity fermions

$$\alpha_{0F}^{\pm}(u) = \alpha_{0F}(0) \pm \beta_0' \sqrt{u} + \alpha_{0F}' u\,. \tag{1.3}$$

Notice that these poles satisfy the condition (1.1) and thus are consistent with the MacDowell symmetry.

In the Reggeon field theory the energy is 1-(angular momentum), and we see that the Pomeron (1.2) plays the role of a nonrelativistic massless particle, while the fermion whose intercept is less than 1 behaves like a particle with nonzero mass. Interaction of a massless particle with a massive one is strongly reminiscent of QED. There it is known[7] that the electron propagator in the infrared limit behaves like

$$G(p^2) = \frac{A(p^2) + \hat{p}B(p^2)}{p^2 - m^2}\,, \quad A, B \sim (p^2 - m^2)^{\beta}. \tag{1.4}$$

This gives us an idea how our exact fermion propagator might be different from what is expected in perturbation theory: In perturbation theory, lowest-order corrections to the bare electron propagator lead to a mass shift, but A, B are still of the form $(p^2 - m^2)^0$, whereas the full renormalized propagator behaves like (1.4), with $\beta \neq 0$. Our case, however, is somewhat more complicated than QED. We have no gauge invariance and our "photon" has a self-interaction.

Using renormalization-group techniques and the ϵ expansion, we find several fixed points which could govern the infrared behavior of our theory. Only two of these turn out to give physically acceptable solutions, but these solutions, in fact, possess a number of rather attractive properties. First, the trajectory of the renormalized fermion is almost linear in u, even though the bare, input trajectory was proportional to $\sqrt{u}$. Although, strictly speaking, we can only draw this conclusion near $u = 0$, this form is in much better agreement with the experimental situation than is the bare trajectory. Second, in addition to these moving singularities, we find, treating the Pomeron-fermion interaction nonperturbatively, that an additional cut is generated in the fermion propagator in the j plane. For $u < 0$, both parity poles are on the physical j-plane sheet, but for $u > 0$, one of them moves onto an unphysical sheet and thus does not show up as a physical particle. Hence, even though the bare theory has physical particles of both parities, the renormalized theory does not.[8] This dynamical mechanism for removing the negative-parity state depends primarily on a certain anomalous dimension being nonintegral. The exact value of this dimension is not important for the argument, and so the mechanism should be valid in most Reggeon field theories, with the possible exception of certain infrared-free theories.

In the course of deriving this result, we first review the Reggeon calculus for fermions and formulate our field theory. Section III describes our renormalization procedure and the renormalization-group equation. In Sec. IV we search for solutions and finally in Sec. V we discuss their physical content.

II. REGGEON FIELD THEORY FOR FERMIONS

In this section we shall formulate the Reggeon field theory for fermions. To this end, we first summarize the Reggeon calculus as discussed by Gribov, Levin, and Migdal in Ref. 5. In particular, we want to repeat their derivation of the fermion propagator.

As is well known, the requirement of Mandelstam analyticity for the A and B amplitudes in π-N scattering leads to a relation between the positive- and negative-parity states in the u channel. For an amplitude described by the exchange of fermion poles, this relation, the MacDowell symmetry, means that the existence of a positive-parity fermion trajectory, α_+, implies the existence of a negative-parity fermion trajectory, α_-, such that

$$\alpha_+(\sqrt{u}) = \alpha_-(-\sqrt{u})\,. \tag{2.1}$$

Now, we can separate the backward π-N scattering amplitude (Fig. 1) into two pieces with definite u-channel parity:

$$T(s,u) = \bar{u}\gamma_5(M^+\Lambda^+ + M^-\Lambda^-)\gamma_5 u\,. \tag{2.2}$$

$\Lambda^{\pm} = \frac{1}{2}(1 \mp \hat{q}_\perp/\sqrt{q^2})$ is the projection operator onto states with definite parity, $\hat{q}_\perp = -\gamma_\perp \cdot q_\perp$, and q is the (transverse momentum) vector perpendicular to the large momenta of the scattering process in the usual Sudakov analysis. $q^2 = -q_\perp{}^2 = u$, so for $u < 0$, $\sqrt{q^2}$ is purely imaginary.

If $M^{\pm}$ are dominated by the exchange of fermion Regge poles,

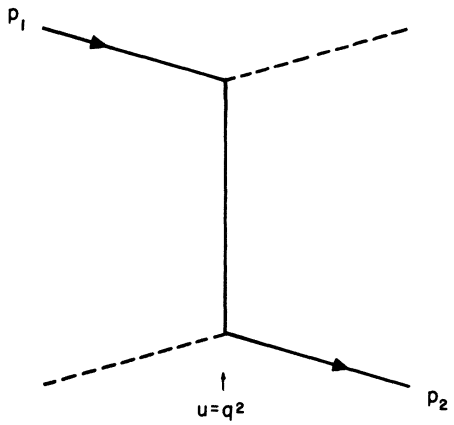

FIG. 1. Backward πN scattering with fermion exchange.

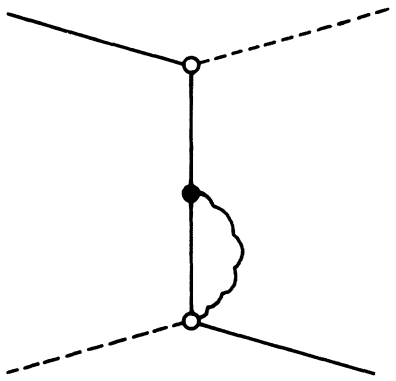

FIG. 2. A Reggeon diagram contributing to Fig. 1. The vertical straight line denotes a Reggeized fermion, the wavy line a Pomeron.

$$M^{\pm} = \eta(\alpha_{\pm}) r^{\pm} \left(\frac{s}{s_0} \right)^{\alpha_{\pm}(\sqrt{u})} . \tag{2.3}$$

η is the signature factor and the residues $r^{\pm}$ are related by

$$r^{+}(\sqrt{u}) = r^{-}(-\sqrt{u}) . \tag{2.4}$$

We can also write $T(s,u)$ in terms of a Mellin transform:

$$T(s,u) = \bar{u}\gamma_5 \frac{1}{2\pi i} \int dj\, \eta(j) s^j f_j(u) \gamma_5 u . \tag{2.5}$$

Then the u-channel partial wave $f_j(u)$ is given by

$$f_j(u) = \frac{r^{+}(\sqrt{u})}{j - \alpha_{+}(\sqrt{u})} \Lambda^{+} + \frac{r^{-}(\sqrt{u})}{j - \alpha_{-}(\sqrt{u})} \Lambda^{-} . \tag{2.6}$$

For real $r^{\pm}$ and for a trajectory of the form

$$\alpha_{\pm}(\sqrt{u}) = 1 - \Delta \pm \beta' \sqrt{u} + \alpha_F' u + \cdots , \tag{2.7}$$

(2.6) can be written as

$$f_j(u) = \frac{r}{j - \alpha(\hat{q})} , \tag{2.8}$$

where

$$\begin{aligned} \alpha(\hat{q}) &= 1 - \Delta_F + \beta' \hat{\boldsymbol{q}} + \alpha_F' \hat{q} \cdot \hat{q} \\ &= 1 - \Delta_F + \beta' \hat{q} + \alpha_F' u . \end{aligned} \tag{2.9}$$

To calculate Regge cuts in the Reggeon calculus arising from the interaction of fermion Regge poles with the Pomeron (an example of which is shown in Fig. 2), one proceeds in much the same way as for boson Regge poles,[1] but in this case, the fermion propagator is

$$i(E + \Delta_{0F} - \beta_0' \hat{q} - \alpha_{0F}' q^2)^{-1} . \tag{2.10}$$

The reader will notice the lovely property that if $\alpha_F' = 0$, (2.10) looks just like a nonrelativistic fermion propagator in ordinary field theory. One could, of course, choose more complicated forms for the fermion propagator, and these will lead to different theories, but (2.10), derived by using a Taylor expansion in $\sqrt{u}$, is the simplest and is the one with which we shall be concerned. Before continuing, there is one additional simplification in (2.10) we want to make. What we want to study by means of the Reggeon field theory is the behavior of the Green's functions for small u. Unless $\beta_0' = 0$, one would expect that the terms of higher order in $\sqrt{u}$ would have little influence on the small-u behavior of the theory. For the pure Pomeron field theory it has been shown[9] that higher-order terms in the bare propagator do not affect the infrared behavior, and this encourages us to expect a similar situation in our theory. Hence, for calculational simplicity, we set $\alpha_{0F}' = 0$ in what follows. It is, however, important to remember that the complete bare fermion propagator is of the form (2.10) with $\alpha_{0F}' \neq 0$. This is necessary if the bare theory is to possess particle poles of negative as well as positive parity and if the bare trajectory is to behave proportional to u for larger u.

The field theory we want to construct will couple a bare Pomeron with a linear trajectory

$$\alpha_{0P} = 1 + \alpha_0' q^2 \tag{2.11a}$$

to a bare fermion whose trajectory can be symbolically written as

$$\alpha_{0F} = 1 - \Delta_{0F} + \beta_0' \hat{q} . \tag{2.11b}$$

Δ_{0F} determines the intercept of the bare trajectory and can be adjusted to give the observed intercept of the renormalized trajectory. In the Reggeon field theory, 1-(angular momentum) plays the role of energy, so from (2.11) we have the energy-momentum relations satisfied by the bare particles: For the Pomeron

$$E = -\alpha_0' q^2 \tag{2.12a}$$

and for the fermion

$$E = -\beta_0' \hat{q} + \Delta_{0F} . \tag{2.12b}$$

Let us now write down the Lagrangian density which governs our field theory. We will then discuss the terms appearing in it.

$$\mathcal{L} = \mathcal{L}_{0P} + \mathcal{L}_{0F} + \mathcal{L}_I , \tag{2.13}$$

with

$$\mathcal{L}_{0P} = \frac{i}{2} \phi^\dagger \overleftrightarrow{\partial}_t \phi - \alpha_0' \vec{\nabla}\phi^\dagger \cdot \vec{\nabla}\phi - \Delta_{0P}\phi^\dagger\phi , \tag{2.14}$$

$$\mathcal{L}_{0F} = \frac{i}{2} \psi^\dagger \overleftrightarrow{\partial}_t \psi - \beta_0' [\psi^\dagger(\not{\partial}\psi) + (\not{\partial}\psi^\dagger)\psi] - \Delta_{0F}\psi^\dagger\psi , \tag{2.15}$$

$$\mathcal{L}_I = -\frac{i\lambda_0}{2}(\phi^\dagger\phi^2 + \phi^{\dagger 2}\phi) + \frac{-ir_0}{2}(\phi\psi^\dagger\psi + \phi^\dagger\psi^\dagger\psi) + \delta\phi\phi^\dagger + \delta_F\psi^\dagger\psi . \tag{2.16}$$

The field $\phi^\dagger$ (ϕ) creates (annihilates) a Pomeron, and $\psi^\dagger$ (ψ) creates (annihilates) a fermion. $\mathcal{L}_{0P}$ ($\mathcal{L}_{0F}$) is the free Lagrangian density for the Pomeron (fermion), and it is not difficult to see that in momentum space these reproduce the correct energy-momentum relations (2.12). $\mathcal{L}_I$ is the interaction Lagrangian and consists of two kinds of terms: three-point functions where a Pomeron may be absorbed or emitted from a Pomeron or fermion line, and mass insertions for both the Pomeron and the fermion. These are adjusted at each order of perturbation theory to give the renormalized trajectory its observed intercept.

The reader will have noticed that our interaction Lagrangian does not allow for the creation or annihilation of fermion pairs. Because Δ_{0F} is strictly positive, closed fermion loops will be unimportant for the small-q^2 (more generally, infrared) behavior of the theory, and so we neglect such terms. (Or, rather, we define our theory without them, since crossing symmetry is not a sacred principle in the Reggeon field theory.) Without these terms, fermion number is conserved through each graph. Hence, we can use the method of Ref. 4 and make a phase change of the fermion field:

$$\psi(\vec{x}, t) \to e^{+i\Delta_{F0}\cdot t}\psi(\vec{x}, t) . \tag{2.17}$$

This formally eliminates Δ_{0F} from our calculations and lets us define a shifted energy

$$\mathcal{E} = E - \Delta_{0F} = 1 - \Delta_{0F} - j , \tag{2.18}$$

which is conserved in graphs with a fermion.

We will want to formulate our field theory in D space and one time dimensions. Physics takes place in the Reggeon field theory at $D = 2$, but more generally we can define the action as

$$A = \int d^D x\, dt\, \mathcal{L}(\vec{x}, t) . \tag{2.19}$$

We will want to study the Green's functions with k fermions entering and leaving the graph, n Pomerons entering, and m Pomerons leaving. These functions, $G^{(k;n,m)}$, are defined by (Fig. 3)

$$G^{(k;n,m)}(E_i, \vec{q}_i; \mathcal{E}_j, \vec{p}_j)\delta\Big(\sum^n E_i + \sum^k \mathcal{E}_j - \sum^m E_i' - \sum^k \mathcal{E}_j'\Big)\delta^D\Big(\sum^n \vec{q}_i + \sum^k \vec{p}_j - \sum^m \vec{q}_i' - \sum^k \vec{p}_j'\Big)$$
$$= \int \prod^n d^D x_i\, dt_i \prod^m d^D x_i'\, dt_i' \prod^k d^D y_j\, dt_j\, d^D y_j'\, dt_j' \exp\Big\{ i\Big[\sum^n (\vec{x}_i \cdot \vec{q}_i - E_i t_i) + \sum^k (\vec{y}_j \cdot \vec{p}_j - \mathcal{E}_j t_j) - \sum^m (\vec{x}_i' \cdot \vec{q}_i' - E_i' t_i') - \sum^k (\vec{y}_j' \cdot \vec{p}_j' - \mathcal{E}_j' t_j') \Big]\Big\}$$
$$\times \langle 0 | T[\phi^\dagger(\vec{x}_1, t_1) \cdots \phi^\dagger(\vec{x}_n, t_n)\phi(\vec{x}_1', t_1') \cdots \phi(\vec{x}_m', t_m')\psi^\dagger(\vec{y}_1, t_1) \cdots \psi^\dagger(\vec{y}_k, t_k)\psi(\vec{y}_1', t_1') \cdots \psi(\vec{y}_k', t_k')] | 0 \rangle . \tag{2.20}$$

For convenience we record here the Feynman rules for construction of the theory in D space dimensions and one time dimension. (From now on, we write always $\vec{q}$ instead of $\vec{q}_\perp$; so $q^2 = -u$.)

1. Draw all topologically distinct diagrams with arrows indicating the direction of propagation of the fermion and the Pomeron.
2. Integrate around each loop $\int d^D k\, dE$.
3. For each triple-Regge vertex, put in a factor $\lambda_0/(2\pi)^{(D+1)/2}$, and, for each Pomeron-Pomeron-

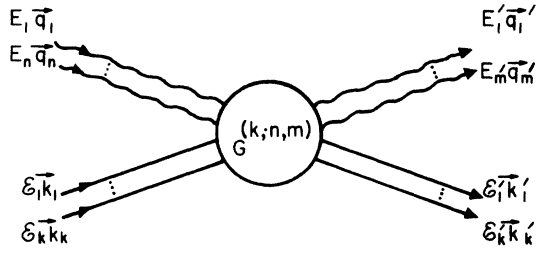

FIG. 3. Definition of $G^{(k;n,m)}$.

fermion coupling, a factor $r_0/(2\pi)^{(D+1)/2}$.

4. For each Pomeron (fermion) mass renormalization counterterm put in a factor $i\delta(i\delta_F)$.

5. For each Pomeron line put in a bare propagator

$$G_0^{(0;1,1)}(E,\vec{q}^2) = i(E - \alpha_0'\vec{q}^2 + i\epsilon)^{-1}.$$

6. For each fermion line put in a bare propagator

$$G_0^{(1;0,0)}(\mathcal{E},\vec{q}) = i(\mathcal{E} + \beta_0'\hat{q} + i\epsilon)^{-1}.$$

7. Put in a factor $\frac{1}{2}$ for each two-Pomeron loop with both momenta in the same direction.

8. Energy and momentum are conserved at all vertices.

Finally, we conclude this section with a dimensional analysis of the quantities which appear in the Lagrangian. Using the condition that ([ ] means dimension of)

$$[A] = E^0 k^0, \tag{2.21}$$

we have

$$[\psi] = [\varphi] = k^{D/2}, \tag{2.22}$$

$$[\lambda_0] = [r_0] = Ek^{-D/2}, \tag{2.23}$$

$$[\alpha_0'] = Ek^{-2},\ [\beta_0'] = Ek^{-1}. \tag{2.24}$$

III. THE RENORMALIZATION-GROUP EQUATIONS

We now want to apply renormalization-group arguments to the connected parts of the Green's functions defined in (2.20). Actually, it is more convenient to work with the amputated connected Green's functions defined as

$$\Gamma_R^{(k;n,m)}(E_i,\vec{q}_i;\mathcal{E}_j,\vec{p}_j) = \left[\prod^n G^{(0;1,1)}(E_i,\vec{q}_i)\prod^m G^{(0;1,1)}(E_i',\vec{q}_i')\prod^k G^{(1;0,0)}(\mathcal{E}_j,\vec{p}_j)\prod^k G^{(1;0,0)}(\mathcal{E}_j',\vec{p}_j')\right]^{-1}$$
$$\times G^{(k;n,m)}(E_i,\vec{q}_i;\mathcal{E}_j,\vec{p}_j). \tag{3.1}$$

Obviously, $\Gamma^{(1;0,0)}$ is just the inverse fermion propagator whose zeros correspond to the j-plane singularities of the fermion propagator. To discuss the backward π-N scattering amplitude, we will also need to consider the Green's functions, $\Gamma^{(1;n,m)}$, which contribute fermion plus Pomeron exchange to the scattering amplitude.

As we mentioned before, the number of fermions is conserved everywhere in each diagram. This leads to the pleasant consequence that Green's functions with no incoming or outgoing fermions are completely independent of the fermions. Hence, the renormalization of the Pomeron propagator and three-point function decouples from the rest of the problem and can be considered separately. This has already been done by Abarbanel and Bronzan,[3] and so we can use their results for this part of our calculation.

Before constructing the renormalization-group equations for $\Gamma^{(k;n,m)}$ we must define our renormalized quantities. For the renormalized Pomeron slope, α', and the triple-Pomeron coupling, λ, we use the definitions of Ref. 3:

$$\Gamma_R^{(0;1,1)}(E,\vec{k}^2)|_{E=0;\,\vec{k}^2=0} = 0, \tag{3.2}$$

$$\frac{\partial i\Gamma_R^{(0;1,1)}}{\partial E}(E,\vec{k}^2)\bigg|_{E=-E_n;\,k^2=0} = 1, \tag{3.3}$$

$$\frac{\partial i\Gamma_R^{(0;1,1)}(E,\vec{k}^2)}{\partial k^2}\bigg|_{E=-E_N;\,k^2=0} = -\alpha'(E_N), \tag{3.4}$$

$$\Gamma_R^{(0;1,2)}(E_1,\vec{k}_1,\ldots,E_3,\vec{k}_3)|_{E_1=2E_2=2E_3=-E_N;\,\vec{k}_i=0} = \frac{\lambda(E_N)}{(2\pi)^{(D+1)/2}}, \tag{3.5}$$

where the normalization point is defined at some negative energy, $-E_N$, with all external momenta set equal to zero. As for the fermion propagator, we require the renormalized trajectory to have its observed intercept Δ_F. In terms of our Green's function, this means

$$\Gamma_R^{(1,0,0)}(\mathcal{E},\vec{k})|_{\mathcal{E}=0;\,k^2=0} = 0. \tag{3.6}$$

For the other renormalization conditions we observe that $\Gamma_R^{(1;0,0)}$ has the matrix structure

$$\Gamma_R^{(1;0,0)}(\mathcal{E},\vec{k}) = \varphi_1(\mathcal{E},\vec{k}^2) + \hat{k}\varphi_2(\mathcal{E},\vec{k}^2). \tag{3.7}$$

In analogy to (3.3), we can require that

$$\frac{\partial i\Gamma_R^{(1;0,0)}(\mathcal{E},\vec{k})}{\partial \mathcal{E}}\bigg|_{\mathcal{E}=-E_N;\,\vec{k}=0} = 1 \tag{3.8}$$

and we can define the renormalized slope, $\beta'(E_N)$, by

$$\frac{\partial i\Gamma_R^{(1;0,0)}(\mathcal{E},\vec{k})}{\partial \hat{k}}\bigg|_{\mathcal{E}=-E_N;\,\vec{k}=0} = \beta'(E_N), \tag{3.9}$$

where

$$\frac{\partial}{\partial \hat{k}} \equiv \frac{1}{D^2}\,\mathrm{Tr}\left(\gamma\cdot\frac{\partial}{\partial k}\right). \tag{3.10}$$

Finally, $r(E_N)$, the renormalized fermion-fermion-

Pomeron coupling constant, is given by

$$\Gamma_R^{(1;\,0,\,1)}(\mathcal{E}_1,\vec{k}_1,\mathcal{E}_2,\vec{k}_2,E_3,\vec{k}_3)\big|_{\mathcal{E}_1=2\mathcal{E}_2=2E_3=-E_N;\ \vec{k}_i=0}=\frac{r(E_N)}{(2\pi)^{(D+1)/2}}\ . \quad (3.11)$$

Now, the Green's functions are multiplicatively renormalized; that is,

$$\Gamma_R^{(k;\,n,\,m)}=Z_P^{(n+m)/2}Z_F^k\Gamma_u^{(k;\,n,\,m)}\ . \quad (3.12)$$

Thus, (3.3) and (3.8) serve to define the Pomeron and fermion wave-function renormalization constants Z_P and Z_F.

All the renormalized Green's functions, Γ_R, are functions of the renormalized parameters, $\alpha'(E_N)$, $\beta'(E_N)$, $\lambda(E_N)$, and $r(E_N)$, as well as the renormalization energy, E_N, and their kinematical arguments, $E_i,\vec{k}_i$. For our purposes, it is convenient to trade in some of these parameters for dimensionless parameters of which the Γ_R may be considered functions. We, therefore, replace λ, r, and β' with the following dimensionless quantities:

$$y(E_N)=\frac{\lambda(E_N)}{[\alpha'(E_N)]^{D/4}}E_N^{(D-4)/4}\ , \quad (3.13)$$

$$h(E_N)=\frac{r(E_N)}{[\alpha'(E_N)]^{D/4}}E_N^{(D-4)/4}\ , \quad (3.14)$$

$$\rho=\frac{\beta'^2(E_N)}{\alpha'(E)E_N}\ . \quad (3.15)$$

Before discussing the renormalization-group equation, we mention a result which will be useful later. Using the dimensional analysis at the end of the last section, and considering Γ_R as a function of ρ, h, and y, we can scale all E's by a, and all k's by b to obtain

$$\Gamma_R^{(k;n,m)}(E_i,\vec{q}_i;\mathcal{E}_j,\vec{k}_j;\rho,\alpha',h,y,E_N)=ab^{(2-2k-n-m)/2}\times\Gamma_R^{(k;\,n,\,m)}\left(\frac{E_i}{a},\frac{\vec{q}_i}{b};\frac{\mathcal{E}_j}{a},\frac{\vec{k}_j}{b},\rho,\frac{\alpha' b^2}{a},h,y,\frac{E_N}{a}\right). \quad (3.16)$$

Now we are ready to write down the renormalization-group equations for the Green's functions. Since the unrenormalized Green's functions are independent of where we have chosen to define the renormalized quantities, they cannot depend on E_N, that is,

$$E_N\frac{\partial}{\partial E_N}\Gamma_u^{(k;\,n,\,m)}\Big|_{\alpha_0',\,\beta_0',\,\lambda_0,\,r_0\ \text{fixed}}=0\ .$$

Using (3.12), the chain rule of differentiation, and remembering that Γ_R are functions of the renormalized parameters, this becomes

$$\left[E_N\frac{\partial}{\partial E_N}+\beta_P(y)\frac{\partial}{\partial y}+\beta_F(y,h,\rho)\frac{\partial}{\partial h}+\Theta(y,h,\rho)\frac{\partial}{\partial\rho}+\zeta(y,\alpha')\frac{\partial}{\partial\alpha'}-k\gamma_F(y,h,\rho)-\frac{m+n}{2}\gamma_P(y)\right]\times\Gamma_R^{(k;\,n,\,m)}(E_i,\vec{k}_i;\rho,\alpha',h,y,E_N)=0\ , \quad (3.17)$$

where

$$\beta_P(y)=E_N\frac{\partial y}{\partial E_N}\ , \quad (3.18)$$

$$\beta_F(y,h,\rho)=E_N\frac{\partial h}{\partial E_N}\ , \quad (3.19)$$

$$\Theta(y,h,\rho)=E_N\frac{\partial\rho}{\partial E_N}\ , \quad (3.20)$$

$$\zeta(y,\alpha')=E_N\frac{\partial\alpha'}{\partial E_N}\ , \quad (3.21)$$

$$\gamma_F(y,h,\rho)=E_N\frac{\partial\ln Z_F}{\partial E_N}\ , \quad (3.22)$$

and

$$\gamma_P(y)=E_N\frac{\partial\ln Z_P}{\partial E_N}\ . \quad (3.23)$$

A brief glance at our dimensional analysis teaches us that, except for ζ, all of these functions are dimensionless, and therefore, can depend only on the dimensionless quantities y, h, and ρ, but not on α'. Moreover, since the Green's functions with $k=0$ decouple from the fermion interaction, the renormalized Pomeron quantities do not depend on the fermion parameters. Hence, β_P, γ_P, and ζ/α' are only functions of y. Notice also that when $k=0$ (3.17) reduces to the renormalization-group equation for the Pomeron Green's functions found in Ref. 3, as it should.

We want to examine the infrared behavior of $\Gamma^{(k;\,n,\,m)}$, in particular $\Gamma^{(1;\,n,\,m)}$, when E_i, $\mathcal{E}\to 0$. We can do this by scaling all energy factors by ξ and considering the limit $\xi\to 0$. Using (3.16), it is easy to derive our equation for $E_N(\partial/\partial E_N)\Gamma_R$ in terms of a derivative with respect to ξ. Eliminating $E_N(\partial/\partial E_N)$ in (3.17) we find for $k=1$

$$\left[-\xi\frac{\partial}{\partial\xi}+\beta_P\frac{\partial}{\partial y}+\beta_F\frac{\partial}{\partial h}+\Theta\frac{\partial}{\partial\rho}+(\zeta-\alpha')\frac{\partial}{\partial\alpha'}+1-\gamma_F-\frac{n+m}{2}\gamma_P\right]\Gamma_R^{(1;\,n,\,m)}(\xi E_i,\vec{k}_i;\rho,\alpha',h,y,E_N)=0\ . \quad (3.24)$$

The parameters α', y, h, and ρ are now to be considered as functions of $t \equiv \ln\xi$. If we introduce the auxiliary functions

$$\tilde{y}(t): \frac{\partial \tilde{y}}{\partial t} = -\beta_P(\tilde{y}(t)), \quad \tilde{y}(0) = y \tag{3.25}$$

$$\tilde{\alpha}'(t): \frac{\partial \tilde{\alpha}'}{\partial t} = \tilde{\alpha}'(t) - \zeta(\tilde{\alpha}'(t), \tilde{y}(t)), \quad \alpha'(0) = \alpha' \tag{3.26}$$

$$\tilde{h}(t): \frac{\partial \tilde{h}}{\partial t} = -\tilde{\beta}_F(\tilde{y}(t), \tilde{h}(t), \tilde{\rho}(t)), \quad \tilde{h}(0) = h \tag{3.27}$$

$$\tilde{\rho}(t): \frac{\partial \tilde{\rho}}{\partial t} = -\Theta(\tilde{y}(t), \tilde{h}(t), \tilde{\rho}(t)), \quad \tilde{\rho}(0) = \rho \tag{3.28}$$

Then the well-known solution to (3.24) can be written as

$$\Gamma_R^{(1;n,m)}(\xi E_i, \vec{k}_i; \rho, \alpha', h, y, E_N) = \Gamma_R^{(1;n,m)}(E_i, \vec{k}_i; \tilde{\rho}(-t), \tilde{\alpha}'(-t), \tilde{h}(-t), \tilde{y}(-t), E_N) \times \exp\left\{ \int_{-t}^{0} dt' \left[1 - \gamma_F(\tilde{y}(t'), \tilde{h}(t'), \tilde{\rho}(t')) - \frac{n+m}{2} \gamma_P(\tilde{y}(t')) \right] \right\}. \tag{3.29}$$

IV. SOLUTIONS OF THE RENORMALIZATION-GROUP EQUATIONS

Without knowing the auxiliary functions, (3.25) to (3.28), it is not possible to determine the behavior of (3.29) as a function of ξ (or t). In particular, the infrared limit $\xi \to 0$ ($t \to -\infty$) may be governed by zeros (Gell-Mann–Low eigenvalues) of the functions β_P, β_F, and Θ. The only technique presently known to learn about such zeros is perturbation theory. *A priori*, it is not obvious that such a perturbation expansion is justified, but if it turns out that a zero of the functions β_P, β_F, and Θ exists for small values of the coupling constants then the perturbation expansion in the neighborhood of this point will be justified *a posteriori*. The analysis in Ref. 3 of the pure Pomeron case, as well as that of Ref. 4 for the ρ-Pomeron field theory, indicates the existence of such zeros for values of the coupling constants of the order of $(4-D)^{1/2} = \sqrt{\epsilon}$. The parameter which seems to determine the accuracy of the approximation, therefore, appears to be ϵ. We proceed with the hope that the infrared behavior in our case will also be governed by coupling constants which are small, in some sense.[10]

To examine this possibility, we need to calculate all the functions appearing in (3.24) to lowest nontrivial order in renormalized perturbation theory, and look for the zeros of β_P, β_F, and Θ. Fortunately, we already know the properties of $\alpha'(t)$ and $y(t)$ from Ref. 3:

$$\gamma_P(y) = -2Ky^2, \tag{4.1}$$

$$\zeta/\alpha' = -2Ky^2, \tag{4.2}$$

$$\beta_P(y) = -y(\tfrac{1}{4}\epsilon - 6Ky^2), \tag{4.3}$$

where

$$K = \left(\frac{\pi}{2}\right)^{D/2} \frac{\Gamma(3 - \frac{1}{2}D)}{4(2\pi)^D}. \tag{4.4}$$

The zero of $\beta_P(y)$ occurs at

$$y_1^2 = 0, \tag{4.5a}$$

$$y_1^2 = \frac{\epsilon}{24K}. \tag{4.5b}$$

In this one-dimensional parameter subspace, (4.5b) is an infrared-stable fixed point because

$$\left.\frac{\partial \beta_P(y)}{\partial y}\right|_{y=y_1} > 0. \tag{4.6}$$

From Ref. 3 we also learn that in the infrared limit ($t \to -\infty$) $\alpha'(t)$ behaves as

$$\alpha'(-t) \sim \alpha' \xi^{-(1+\epsilon/24)}. \tag{4.7}$$

To compute the remaining functions $\beta_F(y, h, \rho)$ and $\Theta(y, h, \rho)$, we have to calculate the graphs of Fig. 4 and use the renormalization conditions (3.7)–(3.11). Because of the spin structure of the fermion the calculations are considerably more involved than in the boson-Pomeron or pure Pomeron case. Nevertheless, after persisting through many hours of tedious calculation we arrive at our results:

$$\gamma_F(y, h, \rho) = \frac{h^2}{(2\pi)^D} \sqrt{\pi}^D \Gamma(1 - \tfrac{1}{2}D) \left\{ \frac{\epsilon}{2} - \frac{\epsilon}{2}\rho^3 \left[\frac{5 + \frac{1}{2}\rho}{8(\rho^2/4 + \rho)^{4/2}} - \frac{\frac{3}{2}}{8(\rho^2/4 + \rho)^{5/2}} \ln \frac{1 + \frac{1}{2}\rho - (\rho^2/4 + \rho)^{1/2}}{1 + \frac{1}{2}\rho + (\rho^2/4 + \rho)^{1/2}} \right] + O(\epsilon^2) \right\}, \tag{4.8}$$

$$\Theta(y, h, \rho) = -\rho \left[1 - y^2 \left(\frac{\pi}{2}\right)^{(D/2)+1} \Gamma(3 - \tfrac{1}{2}D) + 4\pi h^2 \pi^{D/2} \Gamma(1 - \tfrac{1}{2}D) Q_1(\rho) \right], \tag{4.9}$$

$$Q_1(\rho) = -\frac{\epsilon}{32}\frac{3\rho^2(1+\rho)}{(\rho^2/4+\rho)^{5/2}}\ln\frac{1+\frac{1}{2}\rho-(\rho^2/4+\rho)^{1/2}}{1+\frac{1}{2}\rho+(\rho^2/4+\rho)^{1/2}} - \frac{\epsilon}{32}\frac{3\rho^2(2-\rho)}{(\rho^2/4+\rho)^{4/2}} + O(\epsilon^2),$$

$$\beta_F(y,h,\rho) = -\frac{\epsilon}{4}h - \frac{\epsilon}{4}hy^2\left(\frac{\pi}{2}\right)^{(D/2)+1}\Gamma(3-\tfrac{1}{2}D) - 2\pi h^3\pi^{D/2}\Gamma(1-\tfrac{1}{2}D)Q_2(\rho) - 2\pi h^2 y\pi^{D/2}\Gamma(1-\tfrac{1}{2}D)Q_3(\rho), \tag{4.10}$$

$$Q_2(\rho) = -\frac{\epsilon}{2}\left\{2\rho\ln 2 - \rho - \frac{\rho^2}{2}\left[\frac{6+4\rho}{(\rho^2+2\rho)^{2/2}} - \frac{2\rho^2+6\rho+3}{(\rho^2+2\rho)^{3/2}}\ln\frac{1+\rho-(\rho^2+2\rho)^{1/2}}{1+\rho+(\rho^2+2\rho)^{1/2}}\right]\right.$$
$$\left. + \frac{\rho^3}{16}\left[\frac{3\rho^2+21\rho+30}{(\rho^2/4+\rho)^{4/2}} - \frac{\frac{1}{2}\rho^3+5\rho^2+15\rho+9}{(\rho^2/4+\rho)^{5/2}}\ln\frac{1+\frac{1}{2}\rho-(\rho^2/4+\rho)^{1/2}}{1+\frac{1}{2}\rho+(\rho^2/4+\rho)^{1/2}}\right]\right\} + O(\epsilon^2),$$

$$Q_3(\rho) = \frac{\epsilon}{8}\left\{2 - 8\rho\ln 2\left(1+\frac{3}{8(\rho-\frac{9}{4})^2}\right) - 2\rho^2\left[\frac{2\rho^2+6\rho+3}{(\rho^2+2\rho)^{3/2}}\ln\frac{1+\rho-(\rho^2+2\rho)^{1/2}}{1+\rho+(\rho^2+2\rho)^{1/2}} - \frac{6+4\rho}{(\rho^2+2\rho)^{2/2}}\right]\right.$$
$$- \frac{\rho^2}{(\frac{9}{4}-\rho)^2}\frac{1}{(\rho^2/4+\rho)^{2/2}}(2\rho^3 - \tfrac{5}{2}\rho^2 - \tfrac{37}{2}\rho + \tfrac{63}{2})$$
$$\left. + \frac{\rho^2}{2(\rho-\frac{9}{4})^2}\frac{(\rho^4+\frac{3}{2}\rho^3-\frac{257}{8}\rho^2+\frac{1}{2}\rho+\frac{117}{8})}{(\rho^2/4+\rho)^{3/2}}\ln\frac{1+\frac{1}{2}\rho-(\rho^2/4+\rho)^{1/2}}{1+\frac{1}{2}\rho+(\rho^2/4+\rho)^{1/2}}\right\} + O(\epsilon)^2.$$

When we search for a zero of Θ and β_F we must fix y^2 at the value given in (4.5b). The reason is that a fixed point in our three-dimensional parameter space (y, h, ρ) is given by simultaneous zeros of β_P, β_F, and Θ, and the zeros of β_P occur at the values of y^2 given in (4.5). A glance at (4.9) and (4.10) shows that for this value of y^2, given by (14.5b), there is a simultaneous zero of Θ and β_F when

$$\rho_1 = 0, \quad h_1^2 = \left(\frac{y_1}{4}\right)^2 = \frac{\epsilon}{16\times 24K}. \tag{4.11}$$

To see whether the zero is infrared stable, we need to study the matrix

$$\begin{pmatrix} \frac{\partial\beta_F}{\partial h} & \frac{\partial\beta_F}{\partial\rho} \\ \frac{\partial\Theta}{\partial h} & \frac{\partial\Theta}{\partial\rho} \end{pmatrix}. \tag{4.12}$$

A necessary and sufficient condition for infrared stability is that the real parts of both eigenvalues of the matrix (4.12) be positive definite:

$$\mathrm{Re}\lambda_1, \mathrm{Re}\lambda_2 > 0. \tag{4.13}$$

If the renormalized coupling constants lie in a neighborhood of the fixed point, the positivity of the eigenvalues is, in general, required to ensure that

$$y(-t)\to y_1, \quad \rho(-t)\to\rho_1, \quad h(-t)\to h_1 \text{ as } t\to-\infty, \tag{4.14}$$

so that the fixed point dominates the infrared limit.

It can, however, also happen that one or both of the conditions (4.13) are not satisfied. A case of particular interest to our problem is $\lambda_1 > 0$ and $\lambda_2 < 0$, with $\lambda_{1,2}$ real. If in the ρ-h plane $\vec{e}_1$ and $\vec{e}_2$ are the eigenvectors of (4.12) belonging to λ_1, λ_2, respectively, then for h and ρ close enough to (4.11) Eqs. (3.25) and (3.26) can be written as

$$\frac{d}{dt}\begin{pmatrix} h(t)-h_1 \\ \rho(t)-\rho_1 \end{pmatrix} = \begin{pmatrix} \frac{\partial\beta_F}{\partial h} & \frac{\partial\beta_F}{\partial\rho} \\ \frac{\partial\Theta}{\partial h} & \frac{\partial\Theta}{\partial\rho} \end{pmatrix}\begin{pmatrix} h(t)-h_1 \\ \rho(t)-\rho_1 \end{pmatrix} \tag{4.15}$$

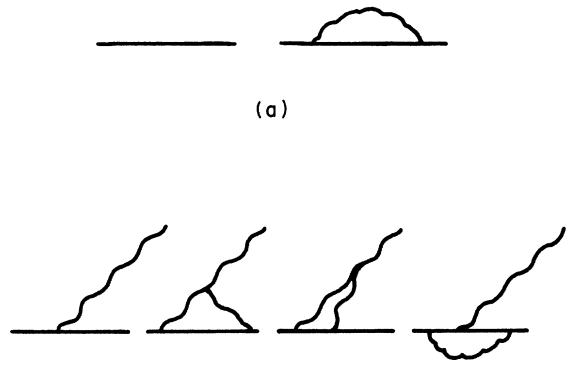

FIG. 4. Lowest-order graphs for (a) $\Gamma^{(1;0,0)}$ and (b) $\Gamma^{(1;0,1)}$.

and the vectors $\binom{h(t)}{\rho(t)}$, $\binom{h_1}{\rho_1}$ decomposed:

$$\begin{pmatrix} h(t) \\ \rho(t) \end{pmatrix} = a(t)\vec{e}_1 + b(t)\vec{e}_2 , \tag{4.16a}$$

$$\begin{pmatrix} h_1 \\ \rho_1 \end{pmatrix} = a_1\vec{e}_1 + b_1\vec{e}_2 . \tag{4.16b}$$

Inserting this into (4.15), we obtain

$$\frac{d}{dt}[a(t)-a_1]\vec{e}_1 + \frac{d}{dt}[b(t)-b_1]\vec{e}_2 = -\lambda_1[a(t)-a_1]\vec{e}_1 - \lambda_2[b(t)-b_1]\vec{e}_2 . \tag{4.17}$$

Since $\vec{e}_1$ and $\vec{e}_2$ are linearly independent,

$$\frac{d}{dt}[a(t)-a_1] = -\lambda_1[a(t)-a_1] , \qquad \frac{d}{dt}[b(t)-b_1] = -\lambda_2[b(t)-b_1] , \tag{4.18}$$

we have the solutions

$$a(t) = a_1 + c_1 e^{-\lambda_1 t} , \quad b(t) = b_1 + d_1 d^{-\lambda_2 t} . \tag{4.19}$$

For $t \to -\infty$, $a(-t) \to a_1$, $b(-t) \to \infty$, while for $t \to \infty$, $a(-t) \to \infty$, $b(-t) \to b_1$. So unless $b_1 = 0$, that is, unless h/ρ lies along the eigenvector $\vec{e}_1$, the infrared behavior is undetermined. Out of the ρ-h plane we see that the condition $b_1 = 0$ corresponds to a plane in the three-dimensional parameter space. Of course, if the renormalized dimensionless parameters choose to lie exactly at the fixed point, the infrared behavior of the theory will be governed by that fixed point regardless of its stability properties. Finally, we mention that if neither condition (4.13) is satisfied, the fixed point can be approached in the infrared limit only along a line in the parameter space perpendicular to the ρ-h plane.

Let us now leave the general discussion and return to the fixed point (4.11). At this fixed point the matrix (4.12) is

$$\begin{pmatrix} \frac{\epsilon}{4} & 0 \\ \frac{\partial\Theta}{\partial h} & -1+\frac{\epsilon}{24} \end{pmatrix} , \tag{4.20}$$

whose eigenvalues are $\epsilon/4$ and $-1+\epsilon/24$. Hence this is an unstable fixed point. The eigenvector belonging to the positive eigenvalue lies along the h axis. Thus, if the physical values of ρ, h, and y are not too far from the fixed point, and moreover, if $\rho = 0$, so that we start on the plane of infrared stability in the three-dimensional parameter space, the Green's functions [using (3.29)] will behave in the infrared limit as

$$\Gamma_R^{(1;n,m)}(\xi E_i, \vec{k}_i, 0, \alpha', h, y, E_N) \underset{\xi\to 0}{\sim} \xi^{1-\gamma_F(y_1,h_1,0)-[(n+m)/2]\gamma_P(y_1)} \times \Gamma_R^{(1;n,m)}(E_i, \vec{k}_i; 0, \alpha'\xi^{-(1+\epsilon/24)}, h_1, y_1, E_N) , \tag{4.21}$$

where

$$\gamma_F(y_1, h_1, 0) = -\frac{\epsilon}{24} , \qquad \gamma_P(y_1) = -\frac{\epsilon}{12} .$$

In the next section we will discuss the physical consequences of the solutions, but first we want to see if there are any other fixed points in our space. Unfortunately, coupled Eqs. (4.9) and (4.10) have a rather complicated dependence on ρ. To discover whether there were any other simultaneous zeros of β_F and Θ, we set $\Theta = 0$, solved for h in terms of ρ, plugged that value of h into β_F, and used a computer to calculate β_F as a function of ρ. Confining ourselves to real values of h and β', we found two more fixed points:

$$(h_2, \rho_2) = (16.1454 \times \tfrac{1}{2}\epsilon, 0.90439) , \tag{4.22}$$

$$(h_3, \rho_3) = (-14.2071 \times \tfrac{1}{2}\epsilon, 1.6048) . \tag{4.23}$$

With sufficient patience one can numerically analyze these fixed points for their stability properties. We have done this, and we find that both fixed points have one negative and one positive eigenvalue. Thus, we have a similar situation as for the fixed point (4.11) and in order to make any statement about the infrared behavior, we must require that our initial values (ρ, h) lie on a certain line in the ρ-h plane (Fig. 5). Viewed in the three-dimensional space (ρ, h, y), this again corresponds to a plane. If the values of the renormalized parameters are such that we approach one of the fixed points (4.22) or (4.23) as $t \to -\infty$, then the infrared behavior of the Green's function will be

$$\Gamma_R^{(1;n,m)}(\xi E_i, \vec{k}_i; \rho, \alpha', h, y, E_N) \underset{\xi\to 0}{\sim} \xi^{1-\gamma_F(y_1,h_j,\rho_j)-[(n+m)/2]\gamma_P(y_1)} \times \Gamma_R^{(1;n,m)}(E_i, \vec{k}_i; \rho_j, \alpha'\xi^{-(1+\epsilon/24)}, h_j, y_1, E_N) \quad (j=2,3) , \tag{4.24}$$

where

$$\gamma_F(y_1, k_2, \rho_2) = -0.649\,188 \times \frac{\epsilon}{2} , \qquad \gamma_F(y_1, h_3, \rho_3) = -0.208\,34 \times \frac{\epsilon}{2} . \tag{4.25}$$

The perverse instability described above which

evidently afflicts all the fixed points in our parameter space has its origin in the fact that the Pomeron and fermion slopes have different dimensions. In the definition of ρ, there is a factor of E_N^{-1}. Differentiating this factor gives a term $-\rho$ in the expression for Θ [Eq. (4.9)]. By examining the matrix A [Eq. (4.12)] it is straightforward to see that this term is responsible for the negative sign of one of the eigenvalues and hence for the instability. Indeed, Fig. 5 shows that the planes of stability are nearly perpendicular to the ρ axis [this is a numerical result for the fixed points (4.22) and (4.23)—in fact, they may be exactly perpendicular. The plane of stability for the fixed point at the origin is exactly perpendicular to the ρ axis.], showing that it is variations in this parameter that give rise to the instability. A different choice for the Pomeron does give rise to stable fixed points in a Pomeron-fermion field theory. This will be discussed elsewhere.[11] Let us now turn to a description of the physical implications of our theory.

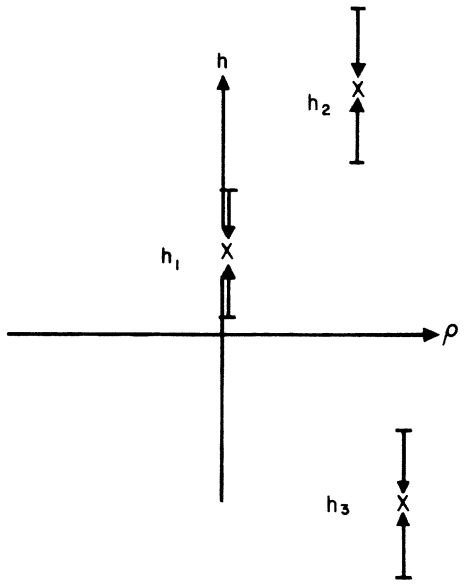

FIG. 5. Fixed points in the h-ρ plane and their infrared-stable eigenvectors.

V. DISCUSSION AND PHYSICAL CONSEQUENCES OF THE SOLUTIONS

Let us now examine in more detail the physical implications of our solutions. We consider first the fixed point (4.11) at which the Green's function is given by (4.21). At this fixed point, $\rho = 0$. Moreover, as we have shown, the only way to approach this fixed point is to start with $\rho = 0$. From Ref. 3 we know that the renormalized Pomeron slope, α', is not infinite, so $\rho = 0 \Rightarrow \beta' = 0$. Now, it is easy to show that to any order in perturbation theory, $\Gamma_R^{(1;\,0,0)}$ depends on $\vec{k}$ only in the combination $\rho^{1/2}\vec{k}$, so for $\rho = 0$ $\Gamma_R^{(1;\,0,0)}$ has no $\vec{k}$ dependence at all to each order in perturbation theory. This indicates that it is likely that the exact renormalized inverse fermion propagator $\Gamma_R^{(1;\,0,0)}$ will have no k-dependent zeros in the $\mathcal{E}$ plane. Hence, the fermion propagator will have no moving j-plane singularities. Since we are looking for a reasonable trajectory with physical fermions, this solution is not very attractive.

Before discussing the other fixed points, we want to mention a very interesting connection between our $\rho = 0$ fixed point and one of the fixed points studied in the ρ-Pomeron field theory of Ref. 4. In a more ambitious study of the fermion-Pomeron problem, we could have included another term in the bare fermion trajectory. In particular, we could have used (2.9) instead of (2.11), and the bare propagator would have been

$$i(\mathcal{E} + \beta_0' \hat{q} - \alpha_{0F}' q^2)^{-1} \tag{5.1}$$

rather than $i(\mathcal{E} + \beta_0' \hat{q})^{-1}$. *A priori*, we do not know whether we would obtain the same fixed points with (5.1) as we did in the present study. On the other hand, if in (5.1) β_0' is set equal to zero, then (5.1) takes the form of a boson trajectory, and we regain the ρ-Pomeron theory studied in Ref. 4. Hence, the field theory of Ref. 4 and the one treated here are special cases of the more general theory obtained using (5.1). There is, however, a qualitative difference in the amount of information lost in the two limits of (5.1) $\beta_0' = 0$ and $\alpha_{0F}' = 0$.

To demonstrate this, we first remark that although in our bare fermion trajectory, $\alpha_{0F}' = 0$, we can still define a renormalized α_F' using

$$\left.\frac{\partial i\Gamma^{(1;\,0,0)}}{\partial q^2}\right|_{\mathcal{E} = -E_N;\; q^2 = 0} = -\alpha_F'(E_N). \tag{5.2}$$

In general this will be nonzero. On the other hand, if $\beta_0' = 0$ as in the ρ-Pomeron theory, the renormalized β' will be identically zero as one can see from its definition (3.10), since the trace of an odd number of γ matrices is zero. Defining $R = \alpha_F'/\alpha'$, we can consider this situation in the three-dimensional parameter space (h, ρ, R) shown in Fig. 6. (There is, of course, a fourth renormalized dimensionless parameter, y, but since the Pomeron renormalization decouples from the secondary trajectory, we need not consider it for the moment.) Since $\beta_0' = 0$ implies $\beta' = 0$, if we start with a boson trajectory we will always be restricted to the R-h plane in the space of renormalized parameters, whereas, since $\alpha_{0F}' = 0 \not\Rightarrow \alpha_F' = 0$, starting with the fermion trajectory we have used will put us someplace in the entire h, ρ, R space. If in

the second case we compute, according to (5.2), the value of $\alpha_F'(E_N)$, $R(E_N)$, and $E_N \partial R(E_N)/\partial E_N$ at our $\rho = 0$ fixed point, we find that $R = E_N \partial R/\partial E_N = 0$. Hence in the ρ-R-h space, this fixed point is on the h axis, and is also a fixed point with respect to variations along the new dimension, R. Furthermore, this fixed point is infrared stable for $\rho = 0$, that is, it is stable against variations in the h-R plane, but it is unstable against variations in ρ (out of the h-R plane).

Starting with $\beta_0' = 0$, the authors of Ref. 4 found a fixed point at $\alpha_F' = 0$ and $h = y_1/4$, which was infrared stable in their parameter space, i.e., in the h-R plane. This is the same fixed point as (4.11) in the present study, but since we must consider variations with respect to ρ, the fixed point is unstable in our (larger) three-dimensional parameter space. Notice also that the other fixed points of Ref. 4 do not appear as fixed points in our problem. Consequently, enlarging the space from that considered in the ρ-Pomeron problem to include variations in ρ qualitatively modifies the solutions. On the other hand, since in our fermion problem $\alpha_{0F}' = 0 \neq \alpha_F' = 0$, adding a term proportional to k^2 in (2.11) with $\beta_0' \neq 0$ does not change the dimensionality of the renormalized parameter space, and so should not qualitatively affect the solutions of the renormalization group equations. These observations further justify our neglect of the term proportional to u in the bare fermion propagator.

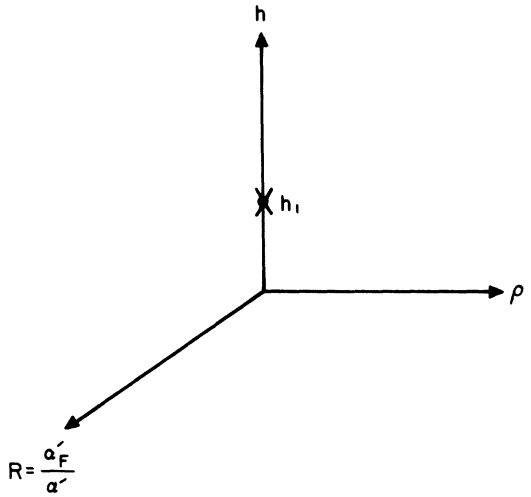

FIG. 6. Three-dimensional space of the renormalized parameters R, ρ, and h. The fixed point at $h = h_1$ is infrared stable in the h-R plane but unstable with respect to variations in ρ.

We continue now and examine the other two fixed points of physical interest, (4.22) and (4.23). Applying the dimensional analysis of Sec. II and (3.15) and writing $\xi = -\mathcal{E}/E_N$ (4.24) becomes

$$\Gamma_R^{(1;0,0)}(\mathcal{E},\vec{k};\rho,\alpha',h,y,E_N) \underset{\xi\to 0}{\sim} E_N\left(\frac{-\mathcal{E}}{E_N}\right)^{1-\gamma_F(y_1,h_j,\rho_j)} \Gamma_R^{(1;0,0)}\left(-1, \frac{\vec{k}\sqrt{\alpha'}}{\sqrt{E_N}}\left(\frac{-\mathcal{E}}{E_N}\right)^{-(1/2)(1+\epsilon/24)}; \rho_j, 1, h_j, y_1, 1\right). \tag{5.3}$$

Using (3.7) we have

$$(5.3) = E_N\left(\frac{-\mathcal{E}}{E_N}\right)^{1-\gamma_F}\left[\phi_1(z) + \frac{\hat{k}}{|k|}\sqrt{z}\,\phi_2(z)\right], \tag{5.4}$$

where

$$z = \frac{k^2\alpha'}{E_N}\left(\frac{-\mathcal{E}}{E_N}\right)^{-(1+\epsilon/24)}, \tag{5.5}$$

and we have suppressed the other arguments y, ρ, and h of ϕ_1 and ϕ_2 since they are just constants. One of the most interesting questions concerns that of the $\mathcal{E}$-plane singularities of the fermion propagator. Using (5.4), we may write the fermion propagator

$$G^{(1;0,0)}(\mathcal{E}_i,\vec{k}) = \frac{1}{E_N(-\mathcal{E}/E_N)^{1-\gamma_F}[\phi_1(z)+\sqrt{z}\,\phi_2(z)]}\Lambda^+ + \frac{1}{E_N(-\mathcal{E}/E_N)^{1-\gamma_F}[\phi_1(z)-\sqrt{z}\,\phi_2(z)]}\Lambda^-. \tag{5.6}$$

The factor $(\mathcal{E}/-E_N)^{1-\gamma_F}$ evidently gives rise to a fixed branch point in the $\mathcal{E}$ plane at $\mathcal{E} = 0$. Other singularities are due to the zeros of $\phi_1 \pm \sqrt{z}\,\phi_2$. Although we do not know the exact form of $\phi_{1,2}$, we do know what the motion of these zeros is for small $\mathcal{E}$. Since $\phi_{1,2}$ depend on $\mathcal{E}$ and k^2 only through z, we know that the trajectory moves like

$$\mathcal{E} \sim \left(\frac{\alpha'}{E_N z_0}k^2\right)^{1/v}, \quad v = 1 + \frac{\epsilon}{24} \tag{5.7}$$

where z_0 is the value of z for which one of the denominators in (5.6) vanishes. Notice that this is the same as the behavior of the Pomeron trajectory.[3] This is a very interesting result from two points of view. First, the renormalized fermion trajectory is almost linear in u which is consistent with its behavior for large u, where it is observed to be approximately proportional to u. Second, the trajectory (5.7) is exactly the same as for the renormalized Pomeron, suggesting

that the Pomeron has a very strong character since in its presence the fermion loses track of what it is, and mimics the behavior of the Pomeron.

Apart from the almost linear u behavior of the trajectory, there is another feature which makes this solution very attractive. We mentioned in Sec. II that the requirements of Mandelstam analyticity forced us to start with a pair of bare fermion trajectories with opposite parities, instead of a single trajectory as in the boson case. However, the particles which should lie on the second (parity doublet) trajectory have not been observed, and no dynamical mechanism has been proposed which successfully explains their absence. We shall now show that the form (5.6) of the propagator quite naturally leads to the disappearance of the parity-doublet state as a physical particle.

Suppose the denominator proportional to Λ^+ in (5.6) vanishes for some z_0:

$$\phi_1(z_0)+\sqrt{z}_0\phi_2(z_0)=0\,. \tag{5.8}$$

In this case we have a trajectory of the form (5.7), and for a real trajectory at positive u (now $k^2<0$) the constant has to be positive and real:

$$\mathcal{E}_+=(Cu)^{1/v}\,,\quad C>0\,. \tag{5.9}$$

Next, we assume (we shall justify this below) that ϕ_1 and ϕ_2 have analytic behavior in z such that

$$\phi_{1,2}(z_0)=\phi_{1,2}(e^{2\pi i}z_0)\,. \tag{5.10}$$

Then we see that for $z=z_0e^{-2\pi i}$ we have a zero of the second denominator of (5.6) since

$$\begin{aligned}\phi_1(z_0e^{-2\pi i})-(e^{-2\pi i}z_0)^{1/2}\,\phi_2(z_0e^{-2\pi i})&=\phi_1(z_0)+\sqrt{z}_0\,\phi_2(z_0)\\&=0\,,\end{aligned} \tag{5.11}$$

and we have a negative-parity pole with the trajectory

$$\mathcal{E}_-=(Ce^{-2\pi i}u)^{1/v}\,. \tag{5.12}$$

[In fact, we not only have one positive- and negative-parity pole, but an infinite number at $\mathcal{E}_{+n}=(Cue^{4\pi in})^{1/v}$, $\mathcal{E}_{-n}=(Cue^{-2\pi i+4\pi in})^{1/v}$. But since v is close to 1 ($v=1+\epsilon/24$), all these poles are far away from each other on different sheets in the $\mathcal{E}$ plane. We shall see that only (5.9) and (5.12) are interesting.]

Now let us consider the location of $\mathcal{E}_+$ and $\mathcal{E}_-$ in the $\mathcal{E}$ plane as a function of u (Fig. 7). For $u>0$, $\mathcal{E}_+$ is real and positive, and describes a trajectory with physical particles. At the same time, $\mathcal{E}_-$ is on another $\mathcal{E}$ sheet (remember the fixed $\mathcal{E}$ cut of the propagator), and does not appear as a trajectory with physical particles for positive u. We now continue to negative u by letting $u\to ue^{i\pi}$. Then the positions of the singularities, $\mathcal{E}_+$, move to

$$\begin{aligned}\mathcal{E}_+(ue^{i\pi})&=(Cu)^{1/v}e^{i\pi/v}\,,\\\mathcal{E}_-(ue^{i\pi})&=(Cu)^{1/v}e^{-i\pi/v}\,.\end{aligned} \tag{5.13}$$

Since $v>1$, $\mathcal{E}_-$ has passed through the cut and is now on the physical sheet. Hence, for $u<0$ there are two complex conjugate trajectories of opposite parity on the physical angular momentum sheet, but when $u>0$, one of them moves through the cut onto an unphysical sheet.

The analyticity properties of our fermion propagator are similar to the analyticity properties found by Carlitz and Kislinger[12] in their scheme of fermion Reggeization. In both their approach and ours, a cut appears in the j plane to hide the negative-parity state. The natures of the cuts are, however, quite different. More importantly, in the approach of Carlitz and Kislinger one assumes *ab initio* the absence of negative-parity particles, while in the present approach we make no such assumptions, but find that they are forced to disappear by the dynamical mechanism of renormalization (interaction with the Pomeron) even though the bare theory possesses such particles.

We now want to justify the assumption we made, (5.10), about the analyticity of $\phi_{1,2}$. We shall do this by examining in detail the first- and second-order terms in an ϵ expansion of these scaling functions. It will become clear that such an expansion is probably valid in the region where we require it. To do this, we first note that at our fixed points, the renormalized coupling constants, y and h, are proportional to $\epsilon^{1/2}$. Thus, in a lowest-nonzero-order ϵ expansion of $\phi_{1,2}$ one need only consider graphs of order h^0 and h^2. Now if we evaluate $\Gamma^{(1;\,0,0)}$ exactly at the fixed point, the solution (5.3) holds for all values of $\mathcal{E}$. Assuming we can make an ϵ expansion of the function $\phi_{1,2}$ we have

$$\begin{aligned}\Gamma_R^{(1;\,0,0)}(\mathcal{E},\vec{k};\rho_j,\alpha',h_j(\epsilon),y_1(\epsilon)E_N)&=E_N\left(\frac{-\mathcal{E}}{E_N}\right)^{1-\gamma_F(y_1,h_j,\rho_j)}\\&\times\left\{\phi_{10}(z)+\epsilon\phi_{11}(z)+O(\epsilon^2)+\frac{\hat{k}}{|k|}\sqrt{z}\,[\,\phi_{20}(z)+\epsilon\phi_{21}(z)+O(\epsilon^2)]\right\}.\end{aligned} \tag{5.14}$$

On the other hand, the left-hand side can be evaluated in second-order renormalized perturbation theory to give

$$\Gamma_R^{(1;0,0)}(\mathcal{E},\vec{k},\dots)=\mathcal{E}+(\rho_j\alpha' E_N)^{1/2}\hat{k}+\epsilon\mathcal{E}\left[G_1\left(\frac{k^2\alpha'}{\mathcal{E}},\frac{\mathcal{E}}{E_N},\rho_j\right)+\frac{\hat{k}}{|k|}\left(\frac{k^2\alpha'}{E_N}\right)^{1/2}G_2\left(\frac{k^2\alpha'}{\mathcal{E}},\frac{\mathcal{E}}{E_N},\rho_j\right)\right], \tag{5.15}$$

where we have dropped the dependence on $h_j(\epsilon)$, $y_1(\epsilon)$. We will not write down the explicit functional form of (5.15) but note only this: If G_1 (G_2) has singularities in $\bar{z}=k^2\alpha'/\mathcal{E}$, then these have to be singularities in $\mathcal{E}$ as well. But from Ref. 5 we know that the graph of Fig. 4(b) has a $\mathcal{E}$ cut at $\alpha' k^2$ and behaves there like $(\mathcal{E}-\alpha' k^2)\ln(\mathcal{E}-\alpha' k^2)$. Therefore, considered as a function of $\bar{z}$, G_1 (G_2) have singularities at $\bar{z}=1$ and behave there like $(|-\bar{z}|\ln|-\bar{z}|)$. Now for $\mathcal{E}\to -E_N$, $z\to\bar{z}$. Comparing (5.14) and (5.15) we obtain

$$\begin{aligned}\phi_1(z)&=-1+\epsilon G_1(-z,\dots),\\ \phi_2(z)&=\sqrt{\rho_j}+\epsilon G_2(-z,\dots).\end{aligned} \tag{5.16}$$

Seeking the zeros of (5.8), we find to first order ϵ

$$z_0=\frac{1}{\sqrt{\rho_j}}+\epsilon\,\text{const}, \tag{5.17}$$

which, as long as the const is not too negative, is far away from $z=-1$, where $\phi_1(z)$ and $\phi_2(z)$ have their singularities. As long as we consider a z_0 which avoids these singularities, we can be reasonably confident in the reliability of the ϵ expansion of $\phi_{1,2}$. Furthermore, since the branch points of $\phi_{1,2}$ in z are not near the origin (see Fig. 8), we can rotate z_0 by $2\pi i$ about the origin, avoiding these singularities. Hence (5.10) will be valid, and this is all we need for the validity of our argument about the disappearance of the parity doublets. It is important to notice that the graphs which contribute to higher orders in the ϵ expansion of $\phi_{1,2}$ only have z-plane singularities further from the origin, and so will not vitiate our arguments. In addition, we stress that we do not require either the ϵ expansion of $\phi_{1,2}$ or analyticity of $\phi_{1,2}$ for all values of z. Our actual requirements are much less stringent.

We now want to discuss the implications of our results for the backward π-N scattering amplitude. In general, there will be contributions to this amplitude from the Green's function $G^{(1;n,m)}$ for all n and m (Fig. 9). Assuming, as usual, that for small u the couplings of the Reggeons to the external particles are constants, and using arguments similar to those of Ref. 3, we have, for the contribution in the $\mathcal{E}$ plane of $G^{(1;n,m)}$ to the backward π-N amplitude,

$$\begin{aligned}I_{n,m}(\mathcal{E},\vec{q})=N_n N_m\int d^D K_1\cdots d^D K_{n+m+2}\,d\mathcal{E}_1 d\mathcal{E}_2\,dE_1\cdots dE_{n+m}\,\delta\Big(\sum^{n}E_i+\mathcal{E}_1-\mathcal{E}\Big)\delta\Big(\sum^{m}E_i+\mathcal{E}_2-\mathcal{E}\Big)\\ \times\delta^D\Big(\sum^{n+1}\vec{K}_i-\vec{q}\Big)\,\delta^D\Big(\sum^{m+1}\vec{K}_i-\vec{q}\Big)\,G_R^{(1;n,m)}(\mathcal{E}_1,\mathcal{E}_2,E_i,\vec{K}_i),\end{aligned} \tag{5.18}$$

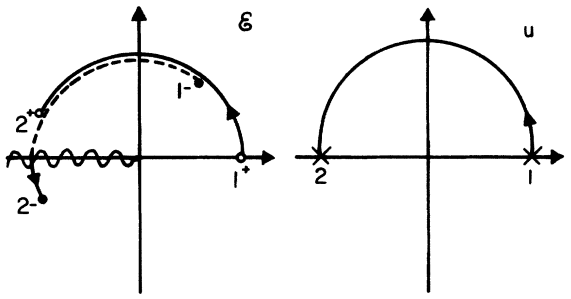

FIG. 7. Location of $\mathcal{E}_+$, $\mathcal{E}_-$ as a function of u. The wavy line in the $\mathcal{E}$ plane denotes the cut in $\mathcal{E}$.

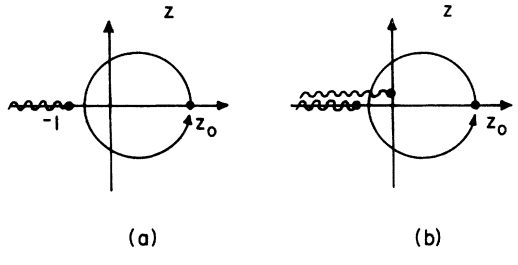

FIG. 8. (a) Analytic structure of $\phi_1(z)$. (b) Analytic structure of $\sqrt{z}\,\phi_2(z)$. Following the paths indicated takes $\phi_1(z_0)\to\phi_1(z_0)$ and $\sqrt{z_0}\,\phi_2(z_0)\to-\sqrt{z_0}\,\phi_2(z_0)$.

which for $\mathcal{E} \to 0$ becomes

$$I_{n,m}(\mathcal{E},\vec{q}) = \mathcal{E}^{-1+\gamma_F}\,\mathcal{E}^{(n+m)[\gamma_P/2+D\nu/4]}\,F_{n,m}(\vec{q}/\mathcal{E}^{\nu/2}). \tag{5.19}$$

Using the values for γ_P, ν at $\epsilon = 2$

$$\gamma_P = -\frac{\epsilon}{12} = -\frac{1}{6}, \quad \nu = 1+\frac{\epsilon}{24} = \frac{13}{12} \tag{5.20}$$

we learn from the Sommerfeld-Watson transform of (5.19) that the leading term is given by $n = m = 0$, i.e., renormalized fermion exchange without Pomerons. Other terms are down roughly by factors of $(\ln s)^{-(n+m)/2}$, so the asymptotic backward π-N amplitude is governed by the renormalized fermion propagator $G^{(1;0,0)}$. This is the same situation encountered in Ref. 3 for forward elastic scattering where the renormalized Pomeron propagator was found to dominate the elastic amplitude. At $u = 0$, our fermion propagator has a cut starting at $\mathcal{E} = 0$, which gives a contribution to the scattering amplitude of the form

$$\sim s^{1-\Delta_F}(\ln s)^{-\gamma_F}. \tag{5.21}$$

For $u < 0$, we have both a branch point at $\mathcal{E} = 0$ and the two complex conjugate moving poles. The fixed-cut contribution behaves like

$$s^{1-\Delta_F}(\ln s)^{-\gamma_F-\nu/2} f(u), \tag{5.22}$$

while the two poles contribute terms

$$s^{1-\Delta_F-\text{const}\times u^{1/\nu}}\eta(\alpha) f(u)\Lambda^{+} + \text{compl. conj.}\times\Lambda^{-}. \tag{5.23}$$

This gives rise to oscillatory behavior proportional to $\cos[c' \ln s\, \mathrm{Im}(u^{1/\nu})]$. However, since ν is close to 1, $\mathrm{Im}(u^{1/\nu})$ is small and the oscillations have a rather long wavelength.

Finally, it is interesting to compare our results with the results obtained by Gribov, Levin, and Migdal,[5] who studied a theory quite similar to the one considered here. These authors assumed a weak-coupling solution for the Pomeron-Pomeron interactions, in which the effective triple-Pomeron coupling vanishes like E when E goes to zero. As a consequence of their belief that such a coupling would be relatively unimportant, they neglected the coupling of the Pomeron to itself and considered a theory in which the Pomeron couples only to the fermion. In such a theory, a Ward identity holds, which relates the fermion Green's function to the fermion-fermion-Pomeron vertex functions. Using this Ward identity, Gribov, Levin, and Migdal were able to predict in their theory the form of the fully renormalized fermion trajectory. They concluded that regardless of whether the solution was for "weak" or "strong" coupling between the Pomeron and the fermion, the exact renormalized fermion trajectory has to be of the form $\mathcal{E} \propto \sqrt{u}$.

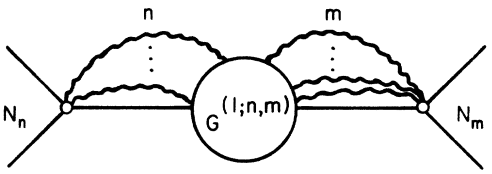

FIG. 9. Scattering amplitude with the exchange of 1 fermion (straight line) and an arbitrary number of Pomerons (wavy lines).

In contrast to this, our theory contains a nonzero Pomeron self-coupling. We know from Ref. 3 that after Pomeron renormalization, the effective triple-Pomeron vertex does not vanish linearly in E but rather like a fractional power of E, and the difference of our result from that of Gribov *et al.* confirms that the Pomeron self-coupling really plays an important role in the renormalization of the fermion trajectory. As to the question whether "weak" or "strong" coupling holds, it is obvious that the renormalized fermion propagator is qualitatively very different from the bare propagator, and so we find no support for the "weak" coupling.

VI. CONCLUSIONS

In our study of a Reggeon field theory with fermions, we have encountered several very interesting properties which we would like to review.

One of the most interesting aspects of this theory is that its behavior at some of the fixed points provides a natural dynamical mechanism to explain the absence of the fermion parity doublets. Even if one chooses, as we have done, a bare fermion propagator with poles on the physical j-plane sheet of both parities, after interaction with the Pomeron, a j-plane cut develops in the renormalized fermion Green's function, and the parity partner moves off the physical sheet for positive u. The major ingredient necessary for this result is the generation of the required j-plane cut. Such a cut is a quite general property of the renormalization procedure, and can be expected to occur in most theories. A possible exception to this is theories in which the fermion is infrared free. In that case, the anomalous dimension at the fixed point is zero, and one must look for weaker branch cuts to hide the fermion parity partner. Depending on the theory, these may or may not be present.

The strong influence of the Pomeron on the fermion trajectory is shown very clearly by another aspect of our theory. Although our bare fermion

trajectory was proportional to $\sqrt{u}$, after interacting with the Pomeron it became roughly proportional to u. This qualitatively different behavior is indeed striking, especially when contrasted with the results of Ref. 5, and shows that, as in many other reactions, any attempt to understand backward π-N scattering must include in a serious way the effects of the Pomeron.

In view of the recent interesting theoretical developments in this area, we would like to modestly suggest that a phenomenology for Reggeon field theories be developed. The reason such a program may hold some promise is that there are many relations implied by these field theories among different renormalized Green's functions. For example, in the theory we have described, the renormalized Pomeron and fermion trajectories have the same behavior near t (or u) = 0. Since the two point renormalized Green's functions are asymptotically the most important, there should be striking similarities in the behavior of near forward elastic scattering and near backward π-N scattering. For example, in our theory, one expects to see oscillations of the form (5.23) in both elastic scattering near $t = 0$ and π-N scattering near $u = 0$. Other field theories will undoubtedly imply similar kinds of relations, some of which may be amenable to experimental verification.

The Reggeon field theory we have studied has produced a number of very interesting physical and mathematical results. The mechanism for ridding the world of fermion parity doublets, the evidence for the strong influence of the Pomeron, and the fact that there are intriguing implications for high-energy phenomenology are all properties of our theory which are expected to be features of most Reggeon field theories. On the other hand, one cannot overlook the fact that none of the fixed points of our theory is infrared stable. Since this instability is most likely due to the different dimensions of the slope parameters of the theory, one may have considerable optimism that this is not a general property of all fermion-Pomeron theories. Indeed, this unwanted characteristic should only induce us to study this rich new approach even further.

ACKNOWLEDGMENTS

We are very grateful to H. Abarbanel, R. Sugar, A. White, and especially J. Bronzan for many enlightening discussions.

APPENDIX

In the appendix we give a short description how to arrive at (4.8)–(4.10). For the calculation of Z_F and $\beta(E_N)$ we compute the graph of Fig. 4(a):

$$i\Gamma_U^{(1;\,0,\,0)}(\mathcal{E},\vec{q}) = \mathcal{E} + \beta_0'\hat{q} - i\left[\frac{r_0}{(2\pi)^{(D+1)/2}}\right]^2 \times \int d^D k\, dE \frac{i}{-E+\beta_0'(\hat{q}-\hat{k})}\,\frac{i}{E-\alpha_0' k^2}. \tag{A1}$$

With the renormalization conditions (3.9) and (3.10) we have

$$\frac{1}{Z_F} = \frac{\partial\, i\Gamma_U^{(1;\,0,\,0)}(\mathcal{E},\vec{q})}{\partial\,\mathcal{E}}\bigg|_{\mathcal{E}=-E_N;\ \vec{q}^2=0} \tag{A2}$$

and

$$\beta'(E_N) = \frac{\partial\, i\Gamma_R^{(1;\,0,\,0)}}{\partial\hat{q}} = Z_F \frac{\partial\, i\Gamma_U^{(1;\,0,\,0)}}{\partial\hat{q}}\bigg|_{-\mathcal{E}=E_N;\ \vec{q}^2=0}. \tag{A3}$$

Within the calculation of the integral of (A1) and the derivatives for (A2) and (A3) the choice of the renormalization point $\vec{q}^2 = 0$ simplifies the work considerably. Moreover, the variable $\rho_0 = \beta_0'^2/\alpha_0' E_N$ turns out to be a natural variable.

For r we have to calculate the graphs of Fig. 4(b):

$$\Gamma_U^{(1;\,0,\,1)}(\mathcal{E},\vec{q},\mathcal{E}_1,\vec{q}_1,E_2,\vec{q}_2) = \frac{r_0}{(2\pi)^{(D-1)/2}} + \frac{r_0^2\lambda_0}{(2\pi)^{3(D+1)/2}}\int d^D k\, dE\, \frac{i}{\mathcal{E}-E+\beta_0'(\hat{q}-\hat{k})}\,\frac{i}{E-\alpha_0' k^2}\,\frac{i}{E-E_2-\alpha_0'(k-q_2)^2+i\epsilon}$$
$$+\frac{r_0^3}{(2\pi)^{3(D+1)/2}}\int d^D k\, dE\, \frac{i}{\mathcal{E}-E+\beta_0'(\hat{q}-\hat{k})}\,\frac{i}{E-\alpha_0' k^2}\,\frac{i}{E_2-E-\alpha_0'(k-q_2)^2+i\epsilon}$$
$$+\frac{r_0^3}{(2\pi)^{3(D+1)/2}}\int d^D k\, dE\, \frac{i}{\mathcal{E}-E+\beta_0'(\hat{q}-\hat{k})}\,\frac{i}{\mathcal{E}_1-E+\beta_0'(\hat{q}_1-\hat{k})}\,\frac{i}{E-\alpha_0' k^2+i\epsilon}. \tag{A4}$$

From this we obtain r by (3.11):

$$\frac{r}{(2\pi)^{(D+1)/2}} = Z_P^{1/2} Z_F \Gamma_U^{(1;\,0,\,1)}(-E_N, 0; -\tfrac{1}{2}E_N, 0; -\tfrac{1}{2}E_N, 0). \tag{A5}$$

All other quantities are built up by direct use of their definitions.

*Present address: Division TH, CERN, CH-1211 Geneva 23, Switzerland.

†Work supported by the Max Kade Foundation.

‡Operated by Universities Research Association Inc. under contract with the United States Atomic Energy Commission.

[1]V. N. Gribov, Zh. Eksp. Teor. Fiz. 53, 654 (1967) [Sov. Phys.—JETP 26, 414 (1968)].

[2]V. N. Gribov and A. A. Migdal, Zh. Eksp. Teor. Fiz. 55, 1498 (1968) [Sov. Phys.—JETP 28, 784 (1969)]; Yad. Fiz. 8, 1002 (1968) [Sov. J. Nucl. Phys. 8, 583 (1969)]; 8, 1213 (1968) [8, 703 (1969)]; V. N. Gribov, E. M. Levin, and A. A. Migdal, *ibid.* 12, 173 (1970) [*ibid.* 12, 93 (1971)]; Zh. Eksp. Teor. Fiz. 59, 2140 (1970) [Sov. Phys.—JETP 32, 1158 (1971)].

[3]H. D. I. Abarbanel and J. B. Bronzan, Phys. Rev. D 9, 2397 (1974).

[4]H. D. I. Abarbanel and R. L. Sugar, Phys. Rev. D 10, 721 (1974).

[5]V. N. Gribov, E. M. Levin, and A. A. Migdal, Yad. Fiz. 11, 673 (1969) [Sov. J. Nucl. Phys. 11, 378 (1970)].

[6]V. N. Gribov, Zh. Eksp. Teor. Fiz. 43, 1529 (1962) [Sov. Phys.—JETP 16, 1080 (1963)]; V. N. Gribov, L. Okun', and I. Pomeranchuk, Zh. Eksp. Teor. Fiz. 45, 1114 (1963) [Sov. Phys.—JETP 18, 769 (1964)].

[7]N. N. Bogoliubov and D. V. Shirkov, *Introduction to the Theory of Quantized Fields* (Wiley-Interscience, New York, 1959).

[8]J. Bartels and R. Savit, Phys. Lett. 56B, 61 (1975).

[9]J. Brower and J. Ellis, Phys. Lett. 51B, 242 (1974).

[10]Calculations of higher-order terms in ϵ carried out by J. Bronzan and J. Dash [Phys. Lett. 51B, 496 (1974)] and M. Baker [*ibid.* 51B, 158 (1974)] for the theory of Ref. 3 do not seem to justify this hope. Indeed, terms of order ϵ^2 are as large as terms of order ϵ. However, one of our most interesting results, namely, the mechanism for the disappearance of the fermion parity doublets does not critically depend on the specific value of the anomalous dimensions of the theory, and is therefore relatively independent of the validity of the first-order ϵ expansion.

[11]R. Savit (unpublished).

[12]R. Carlitz and M. Kislinger, Phys. Rev. Lett. 24, 186 (1970).